INVESTIGATION ON THE INFLUENCE OF DIFFERENT MODELING OF MULTIPLE SURFACE LAYERS ON A 3D TOPOLOGY OPTIMIZATION

Jan Holoch, M.Sc., Sven Lenhardt, M.Sc., Robert Renz, M.Sc., Univ.-Prof. Dr.-Ing. Dr. h. c. Albert Albers
(IPEK – Institute of Product Engineering, Karlsruhe Institute of Technology (KIT));

Abstract

Products nowadays are expected to have load-compliant designs as well as a high degree of individuality and design flexibility. In this context, topology optimization in combination with a redesign provides a possibility to generate load-compliant product designs. In terms of achieving a high individuality and design flexibility additive manufacturing processes like selective laser melting (SLM) can be used.
SLM is an additive manufacturing process that creates a part layer by layer and each one in two steps. First, the outer contour is formed and afterwards the inner area. This separation ensures that a comparatively high contour accuracy is realized. However, at the same time it results in three areas (contour, interface and hatching) with different material properties due to different cooling rates.
To consider these areas including their material properties in a topology optimization, a method is developed to interrupt the topology optimization after each iteration and export the smoothed interim result. Subsequently, the exported interim result is automatically divided into the three areas by offsets using the level set method.
In this contribution, a 3D topology optimization is investigated that assigns different isotropic material properties to the corresponding areas after each iteration. After this assignment, the optimization is continued and the described procedure is repeated until the optimization fulfils its convergence criterion. Thus, the influence of such an interruption and change of material properties on the result of the topology optimization is analyzed on a simple part.
The results depict, that the methodology tries to maximize the surface area, if Young's modulus of the contour area is higher in comparison to the hatching area and if Young's modulus in the interface area is lower in comparison to the hatching area. In the future, the method will be extended to include experimentally measured material properties of the SLM process.

1. Introduction

Today, the trend is to manufacture products more individually and with greater design flexibility, while ensuring a load-compliant structure [1]. Additive manufacturing (AM) processes such as selective laser melting (SLM), which create components in a layer-wise process, are suitable for this purpose. SLM does not require any shaping tools, which gives it a high degree of design flexibility compared to conventional manufacturing processes. [2] Therefore, SLM enables the production of load-compliant structures, which are mostly reflected in complex components, as well as high material utilization [3]. In order to determine such load-compliant structures for a given load case, a topology optimization is often used. Combining SLM with such a topology optimization represents an opportunity to generate simulative supported load-compliant product designs in early phases of product development, while considering the manufacturing process. Therefore, a topology optimization method is currently in development with the aim of considering the material properties induced by SLM as well as applying them during the optimization.

2. State of the Art

Selective Laser Melting

SLM is a powder bed-based AM process, which produces components layer by layer. For each printing layer (see Figure 1 a)) powder is applied and subsequently melted by a laser in two steps. First, the surface (contour area) is melted and consolidated, while the inner area (hatching area) is processed in the second step. This systematic procedure achieves a comparatively high contour accuracy. [4] Simultaneously, it causes porosity due to locally different cooling rates within the component at industrially relevant process speeds [5]. This porosity arises particularly in the so-called interface area, located between the contour area and the hatching area. In comparison, significantly less porosity occurs in the hatching area and almost none in the contour area (see Figure 1 b)). [6]

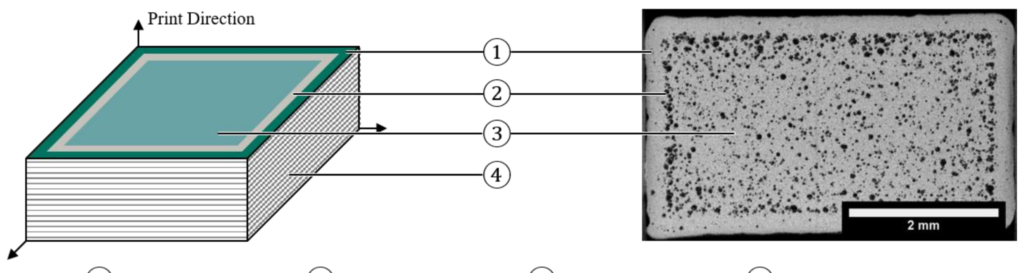

a) Exemplary representation of the three porous areas

b) CT scan to visualize the porosity distribution

Figure 1: SLM-specific porosity distribution and the resulting areas

As a result, SLM creates three areas (contour, interface and hatching) that have different porosity distributions, which in turn lead to varying elastic material properties. In this context, an increasing porosity leads to a reduction in elastic material properties (Young's modulus and shear modulus).

Topology Optimization

In order to generate an initial design for the load-compliant structure of a component, commonly computer-aided methods such as topology optimization are used. Latter is based on the finite element method (FEM) and enables the identification of load paths within a given design area. The elements in this design area are iteratively adjusted during the individual optimization cycles in such a way that the result of the topology optimization is a load-compliant component structure with a simultaneous reduction in volume. [7] In density-based topology optimization, two different approaches can be used in order to maximize or minimize an objective function, e.g. maximizing stiffness for a given volume reduction. The optimality criteria-based approach relies on the use of an optimality criterion that is specifically defined for a given objective function. The sensitivity-based approach, on the other hand, is based on the calculation and evaluation of sensitivities. Its advantage lies in the fact that additional restrictions such as a minimum wall thickness or a global strength restriction can be taken into account within the same optimization problem. [8] Both approaches share that their material models are mostly isotropic and homogeneously distributed across the component [9].

Level-Set Method

The level set method represents a numerical method for the representation and tracking of moving interfaces [10]. Thereby, the interface is represented as a zero-level set (points with value equal zero) of a scalar function in higher dimension, which is called the level set function (LSF). The interface, for example, can represent a curve in 2D or a surface in 3D. An advantage of the level set method is modeling the interfaces with implicit functions, which automatically handles phenomena in the topology of the moving interface, such as intersections. [11] Thus, no additional revision of the interface is necessary compared to an explicit description. A very frequently used LSF is the signed distance function (SDF), which represents at each point the signed distance to the interface. The sign of the SDF indicates whether the point is inside or outside the zero-level set. [12]

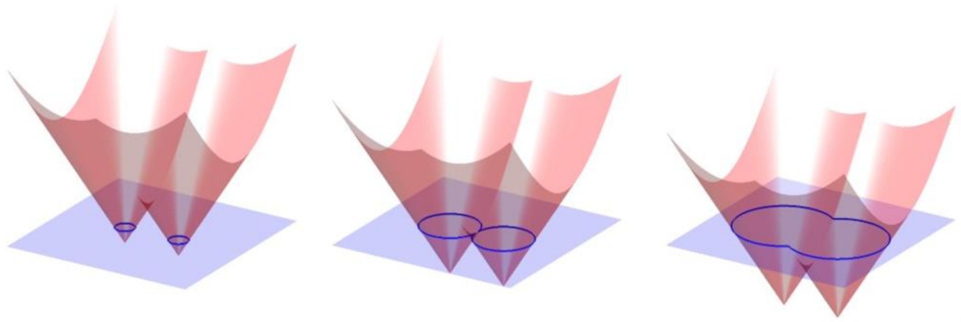

a) Initial interface (zero-level set) *b) Propagating interface* *c) Further propagating interface*

Figure 2: Level set representation of a propagating 2D interface (blue line) with SDF (red) according to [11]

Figure 2 illustrates the principle of the level set method by means of a propagating interface in 2D, which initially consists of two circles (see Figure 2 a)). The interface is illustrated as a blue line and propagates in the normal direction (see Figure 2 b) und c)). As Figure 2 b) und c) show, there are no overlapping circles, but interfaces adapted to the topology. Thus, with the use of the SDF it is possible to generate isolines in 2D or isosurfaces in 3D, which automatically consider phenomena like intersections in the topology.

3. Aim of Research

While SLM has great potential in terms of design flexibility, the systematic approach to the manufacturing process results in three areas in the component with varying porosity. This has a negative effect on the elastic material properties and thus the overall stiffness of the SLM component. Furthermore, this leads to the fact that there is not a homogeneous material distribution in the entire component, instead only locally in the respective three areas. As a result, it is not possible to consider the material properties directly in a standard topology optimization. It is therefore necessary to develop an optimization method that considers the three porous areas and the associated material properties during topology optimization in each design cycle. Hereby these material properties are included in the calculation of the objective function. Through this consideration, the synergies between SLM and topology optimization can be used in a constructive manner. The basic structure of the optimization method is already developed for 2D components, but considering only two instead of three porous areas [13]. This article therefore focuses on the extension of the optimization method to 3D components and the consideration of the three porous areas described. Furthermore, the influence of different parameters such as the additional consideration of a minimum wall thickness is investigated and the effect on the optimization results analyzed.

4. 3D-Topology Optimization Method

In order to include the influence of the porous areas caused by SLM and thus varying material properties in a topology optimization, the 2D optimization method was further developed to 3D components. To ensure that the varying material properties can be integrated during the topology optimization running in Abaqus, it is necessary to interrupt the optimization in every design cycle [14]. During this interruption, three steps are performed, which allow an iterative consideration of the three porous areas and associated material properties:

1. Exporting the smoothed interim result of the current optimization iteration.
2. Generate the three porous areas by calculating two offsets using a SDF and assigning the material properties to the areas.
3. Mapping these material properties to the initial topology optimization mesh.

In the first step, the smoothed surface of the interim result of the current optimization iteration is exported, resulting in a triangle mesh in Standard Triangulation Language (STL) format (see Figure 3 a)).

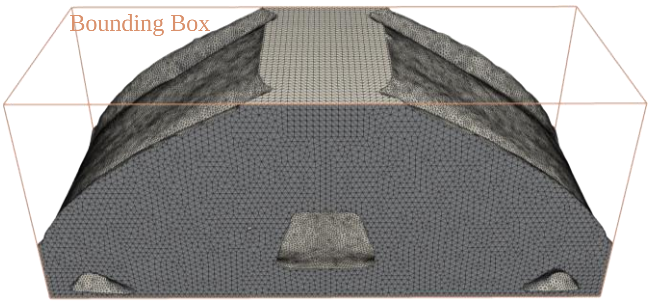

a) Smoothed interim result of the current optimization iteration including the bounding box

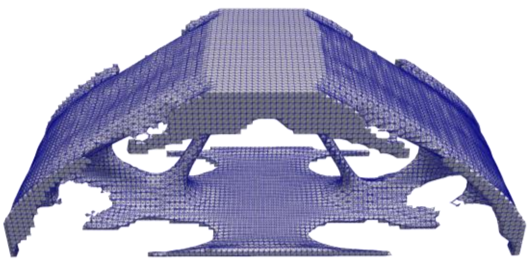

b) Offset 1

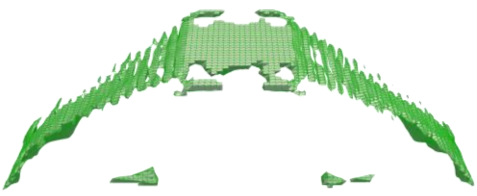

c) Offset 2

Figure 3: Creation of the offsets

In the second step, the boundaries of the three areas, i.e. between contour and interface area (offset 1) and between interface and hatching area (offset 2) are calculated. Therefore a spatial grid is created within a bounding box, which is placed around the smoothed surface mesh from step one (see Figure 3 a)). To compute the SDF, the distance of each grid point from the surface mesh is calculated. For this calculation of the SDF, it is necessary to capture the distance between a point in space and a triangle [15]. In addition, the sign of the SDF, which indicates whether a point is inside or outside the smoothed geometry, must be determined. For this purpose the principle of the Winding Numbers is used [16]. Using the signed distance calculated in this way for each grid point to the nearest triangle, the surface meshes of the two offsets can be generated based on the resulting signed distance field (see Figure 3 b) and c)). These are generated using the Marching Tetrahedra (MT) algorithm [17].

After the surface meshes (smoothed interim result and offsets) are created (see Figure 4 a)), the areas between them are meshed with tetrahedral elements. Subsequently, the generated tetrahedral elements are assigned to the three areas (see Figure 4 b)) and the material properties within them are determined.

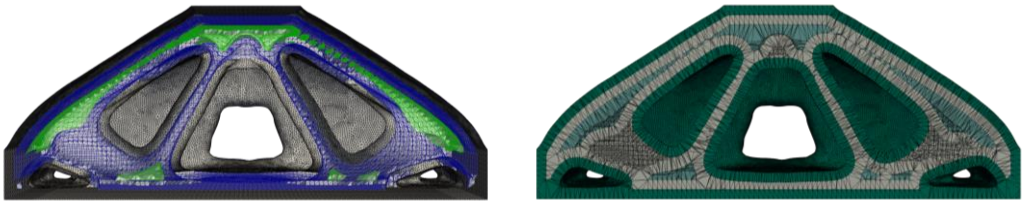

a) Surface meshes: Smoothed interim result (black), Offset 1 (blue) and Offset 2 (green)

b) Meshing and assigning of the porous areas: Contour (dark green), Interface (grey) and Hatching (light green)

Figure 4: Generation, meshing and assigning of the SLM-specific porous areas on the basis of the smoothed interim result

In order to consider the SLM-specific material properties in the respective areas of the finite element analysis (FEA) of the topology optimization, in the third step of the interruption these material properties are mapped from the FE mesh generated in step two (see Figure 5 a)) to the initial FE mesh of the topology optimization.

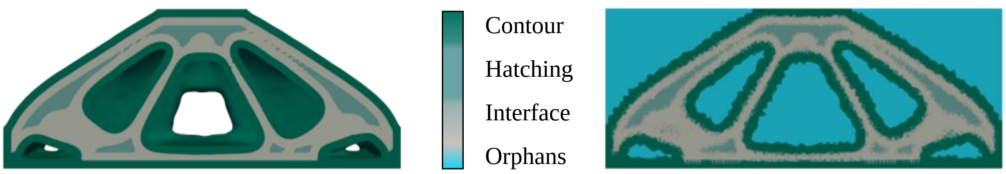

a) In step two created FE mesh

b) Initial FE mesh of the topology optimization

Figure 5: Sectional view of the material properties mapped via MapLib during topology optimization

Therefore, the mapper software MapLib of Fraunhofer Institute for Algorithms and Scientific Computing (SCAI) is used [18]. As a result, the initial FE mesh of the topology optimization is provided with the Young's moduli of the individual elements (see Figure 5 b)). Elements (orphans), which are shown in cyan in Figure 5 b), get an E-modulus which is approximately 0, because they do not contribute to the load conduction and have already been eliminated by the optimization.

The described three steps are performed in each iteration of the topology optimization and thus the three areas created by the SLM are taken into account. These three steps are carried out until the optimization reaches a convergence criterion or a maximum number of iterations.

5. Results and Discussion

Modeling Setup

A simple bending beam serves as the FE model for investigating the influence of the three porous areas in the topology optimization. The beam consists of a fixed-loose bearing at the lower side edges and a predefined displacement d of 0.2 mm of all nodes in the center of the upper surface (see Figure 6).

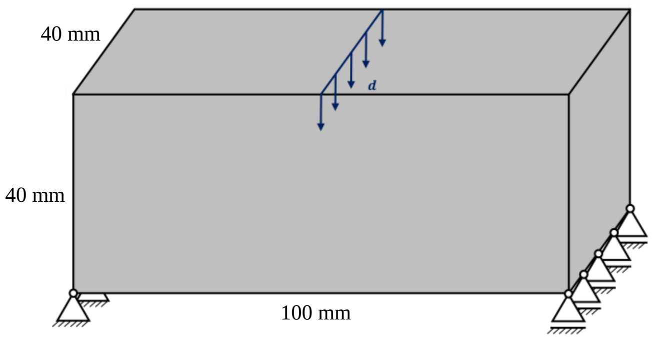

Figure 6: 3-point bending beam including dimensions, clamping and loading

The sensitivity-based optimization approach is chosen since it provides a greater choice of objective functions. As meshing, tetrahedral elements with a quadratic basis function are selected to compensate the stiffening effect of the tetrahedral elements. The global element edge length is 1.0 mm, since the contour and interface areas are specified with a thickness of 2.0 mm each. By choosing 1.0 mm as the element edge length, it is possible to ensure that there are at least two elements in each of the areas across the thickness. AlSi10Mg with a Young's modulus of 70 GPa, a poisson ratio of 0.35 and hence a shear modulus of 26 GPa is used as the material in the hatching area. The contour area has an approximately 10 % higher Young's modulus and shear modulus (77 GPa and 28.5 GPa) and the interface area has an approximately 8 % lower Young's modulus and shear modulus (64.5 GPa and 24 GPa). This correlation was derived from material characterization experiments. Since this paper focuses on the fundamental influence of the iterative consideration of the three areas, the respective material properties are assumed isotropic.

Optimization Parameters

The objective function of the optimization represents the maximization of the stiffness at a given volume reduction to a relative final volume of 40 %. The following two cases are investigated:

Optimization case 1: Maximization of the stiffness
Optimization case 2: Maximization of the stiffness while considering a minimum wall thickness

In optimization case 2 the minimum wall thickness is defined as 9 mm. This thickness results from the assumption that all three porous areas must prevail at every point of the component. This means that a closed volume over its thickness must always consists of the three porous areas in the following order: Contour, interface, hatching, interface and contour (see Figure 1 a)). Both optimization cases are carried out with the iterative consideration of the three porous areas including their associated material properties by using the developed 3D topology optimization method as well as without their consideration, by means of a standard topology optimization. The latter receives the isotropic material properties of the hatching area as input.

Static FE-Analysis

In order to compare the results of the topology optimization quantitatively, each topology optimization is followed by a static FE-Analysis under the same boundary conditions and loads. The resulting designs, including porous areas and associated material properties of the topology optimization (see Figure 7 a)) are transferred to the FE mesh of the static analysis (see Figure 7 b)) using MapLib.

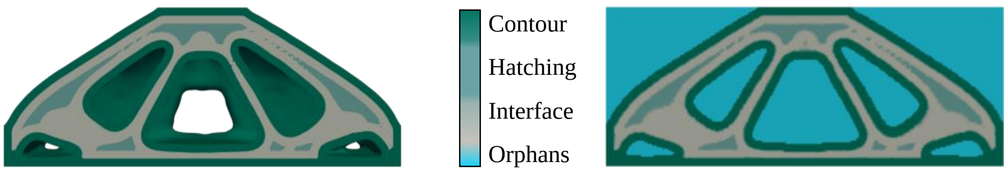

a) Mesh containing the porous areas basing on the result of the topology optimization

b) Mesh for the static FE-Analysis

Figure 7: Sectional view of the material properties transferred via MapLib for the static analysis

Compared to the initial mesh, the mesh for the static analysis is significantly finer in order to reduce inaccuracies through mapping. The designs of the standard topology optimization also contain these porous areas as well as their associated material properties to map the manufacturing process as well. Here, the mapping is the same as described in chapter 4. For quantitative comparison of the designs from the topology optimizations, the strain energy is used, which corresponds to the elastic energy absorbed by the system. For a given displacement, a higher strain energy is equivalent to greater component stiffness.

Optimization Results

In the following, the results of the two optimization cases are presented. In each case, the resulting designs of the topology optimization considering the porous areas as well as the standard topology optimization are compared and discussed, taking into account the results from the static FE analyses. It should be noted that Figure 8 b) and Figure 9 b) already contain the material assignments of the three areas (contour: dark green, interface: gray, hatching: light green) required for the static FE analyses, even if these are not considered in the standard topology optimization itself. They serve the purpose of better illustration and evaluation.

First, the resulting designs of optimization case 1 for the topology optimization considering the porous areas (see Figure 8 a)) and the standard topology optimization (see Figure 8 b)) are visualized and discussed.

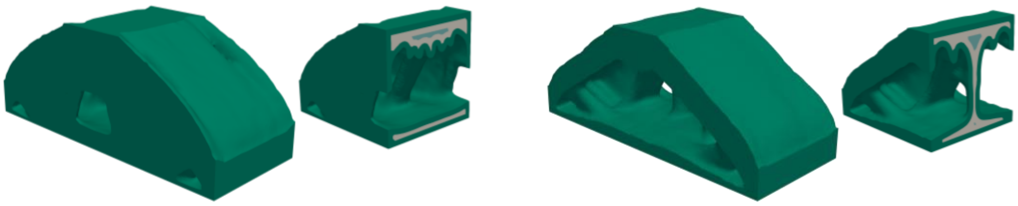

a) Iterative consideration of the porous areas in the topology optimization (full and sectional view)

b) Standard topology optimization (full and sectional view)

Figure 8: Resulting designs for optimization case 1 including the porous areas

Considering the standard topology optimization, it shows that a kind of double-T beam (see sectional view Figure 8 b)) appears in the center as well as locally distributed struts. This is due to the uniaxial bending load case and reflects a conventional design for bending loads. In contrast, the results of the optimization considering the porous areas iteratively indicate that a kind of hollow profile results. This becomes particularly apparent on the long sides of the beam. In addition, this optimization results in the formation of a rib-like structure on the upper inside (see sectional view Figure 8 a)) of the beam. This, like the hollow profile, contributes to an increase in the surface area and thus to more material in the contour area. The increased surface area is a result of the improved material properties in the contour area and is therefore preferred by the optimizer. Along with the qualitative analysis of the surface, the quantitative evaluation of the percentages of the three areas in the overall volume shows that the contour area is about 6% larger and the interface area about 6% smaller, taking porous areas into account, compared to the standard optimization. The volume fraction of the hatching area is equal in both results.

Therefore, it can be stated that in optimization case 1, the contour area is maximized while the interface area is minimized. This approach of the optimizer implies plausibility, since improved material properties lead to improved overall stiffness. This effect of the improved overall stiffness becomes clear through the static analysis. For the volume-specific strain energy $[mJ/mm^3]$, the overall stiffness of the optimized beam considering the porous areas increases by about 1.5 %. The material input is the same for both optimizations and the improvement in stiffness derives from the targeted distribution of the porous areas in the beam.

However, as a result of the restriction-free optimization and the associated maximization of the surface, there are numerous regions in the beam that are exclusively assigned to the contour area. Due to this, the three areas created in the SLM are not maintained in the entire beam and thus do not reflect the manufacturing process. To prevent or limit this deviation, a minimum wall thickness of 9 mm is defined in optimization case 2 (see Chapter *Optimization Parameters*). The aim is to ensure that all three porous areas occur across the cross-section.

The effect of a minimum wall thickness is reflected in optimization case 2 and shows the resulting design of the beam considering the porous areas (see Figure 9 a)) as well as the standard topology optimization (see Figure 9 b)).

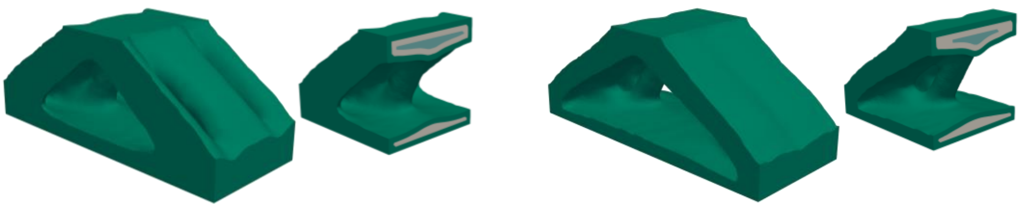

a) Iterative consideration of the porous areas in the topology optimization (full and sectional view)

b) Standard topology optimization (full and sectional view)

Figure 9: Resulting designs for optimization case 2 including the porous areas

It is striking that the difference between the resulting designs is significantly smaller than in optimization case 1. Both designs have a kind of truss structure in which the applied force is dissipated directly into the mounts and are similar to the result in Figure 8 b), but without vertical struts in the center of the beam. The main difference between the designs in Figure 9 consists in the fact that the optimizer still tries to maximize the surface when considering the porous areas. This becomes clear, for example, when the top of the beam has indentations (see Figure 9 a)), whereas the standard topology optimization produces a smooth surface. As before, this is supported by a quantitative evaluation of the percentage shares of the three areas in the overall volume. The design from Figure 9 a) has about 6 % more contour area and about 6 % less interface area compared to Figure 9 b). However, it is noticeable that the hatching area in this optimization case is 10 % larger than in optimization case 1 and is caused by the specified minimum wall thickness.

The static analysis of the two designs shows that the results are also closer to each other here, with an approximately 1.0 % higher weight-specific strain energy when the porous areas are taken into account. Therefore, it can be stated that by choosing a minimum wall thickness, the design freedom is limited in such a way that the optimizer has less possibilities to increase the surface. This has a detrimental effect on the increase in overall stiffness compared to a standard topology optimization with the same material input. This effect can be explained on the basis of the selected parameters. By choosing a volume reduction of 60 % and at the same time limiting the minimum wall thickness to 9 mm, the optimizer retains fewer options, since the main load path must first be filled with material. With the selected dimensions of the beam, this takes up a large part of the available volume and thus limits the possibilities of the optimizer.

Therefore, in the future, further parameter investigations will be carried out with regard to the volume reduction as well as the minimum wall thickness. In addition, the selected combination of volume reduction and minimum wall thickness in conjunction with the rather coarsely selected areas (contour and interface) explain why the hatching area is not or only partially present in the lower area of the two bars (see sectional view Figure 9). Here, the optimizer lacks available volume. However, this effect can be circumvented, for example, by a thinner choice of the porous areas or a lower volume reduction and will be adapted in the future to the thicknesses of the areas derived from experimental tests. The minimum wall thickness thus represents a way of taking the three porous areas in the optimization method into account in order to represent the manufacturing process.

6. Conclusion and Outlook

SLM offers a high degree of design flexibility, but it also entails three porous areas in the final component. In order to consider these in the early stages of product development when choosing a product design, this article presents an optimization method. The porous areas including their material properties, assumed to be isotropic in this article, are iteratively considered in a topology optimization. For this purpose, it is necessary to interrupt the optimization after each iteration and export the smoothed interim result. Subsequently, the calculation of the three porous areas as well as the assignment of their material properties is carried out. Finally, the material properties are mapped to the original optimization mesh to be available to the optimizer for the calculation of the next iteration.

The article shows that by the presented method the specific consideration of the areas can be reliably applied to arbitrary components. The consideration leads to a maximization of the components surface. This results in stiffer designs using the same amount of material compared to a standard topology optimization. In order to always have all three porous areas present in the optimization, the restriction of a minimum wall thickness can be introduced. Here, the surface area is still maximized, resulting also in a stiffer overall design. However, this restriction leads to a limitation in the freedom of the optimizer and the stiffness increase turns out to be smaller. Furthermore, a dependence of the resulting designs on the selected parameters volume reduction and minimum wall thickness is evident. These parameters will be examined in more detail in future studies and their effect on the stiffness increase will be investigated.

In addition, the material properties of the porous areas will not be assumed isotropic in the future, but will be modeled with the results from experimental tests. Also, overhangs will be considered and modeled separately. Furthermore, a strength restriction will be introduced in the optimization and its effect on the resulting designs investigated.

7. References

[1] Brecher, C., Kozielski, S., and Schapp, L. (2011). *Integrative Produktionstechnik für Hochlohnländer*: In: Wertschöpfung und Beschäftigung in Deutschland: Springer. 47–70.

[2] Thompson, M. K., Moroni, G., Vaneker, T., Fadel, G., Campbell, R. I., Gibson, I., Bernard, A., Schulz, J., Graf, P., and Ahuja, B. (2016). *Design for Additive Manufacturing. Trends, opportunities, considerations, and constraints*: In: CIRP annals 65, 2. 737–760.

[3] Lippert, R. B. (2018). *Restriktionsgerechtes Gestalten gewichtsoptimierter Strukturbauteile für das selektive Laserstrahlschmelzen*: TEWISS Verlag.

[4] Gebhardt, A. (2016). *Additive Fertigungsverfahren. Additive Manufacturing und 3D-Drucken für Prototyping - Tooling - Produktion*: Hanser.

[5] Kruth, J.-P., Ed. (2010). *Part and material properties in selective laser melting of metals*: SHANGHAI JIAO TONG UNIV PRESS.

[6] Holoch, J., Czink, S., Spadinger, M., Dietrich, S., Schulze, V., and Albers, A. (2020). *SLM-Topo. Prozessspezifische Topologieoptimierungsmethode für im Selektiven Laserschmelzen gefertigte Leichtbaustrukturen*: In: Industrie 4.0 Management (04). 45–49.

[7] Bendsøe, M. P. and Sigmund, O. (2003). *Topology Optimization. Theory, Methods and Applications*: Springer Science & Business Media.

[8] Dassault Systèmes (2017). *SIMULIA User Assistance 2017*. https://abaqus-docs.mit.edu/2017/English/DSSIMULIA_Established.htm. Accessed 10 July 2021.

[9] Harzheim, L. (2014). *Strukturoptimierung. Grundlagen und Anwendungen*: Verlag Europa-Lehrmittel.

[10] Osher, S. and Fedkiw, R. P. (2003). *Level Set Methods and Dynamic Implicit Surfaces* 153: Springer.

[11] Gibou, F., Fedkiw, R., and Osher, S. (2018). *A Review of Level-Set Methods and Some Recent Applications*: In: Journal of Computational Physics 353. 82–109.

[12] Khoei, A. R. (2015). *Extended Finite Element Method. Theory and applications*: Wiley.

[13] Holoch, J., Träger, L., and Albers, A. (2020). *SLM-Topo - Einfluss unterschiedlicher Modellierung von Randschicht und innerem Volumen auf eine 2D-Topologieoptimierung*: In: NAFEMS Virtuelle DACH Konferenz. 106–109.

[14] Albers, A., Holoch, J., Dietrich, S., and Spadinger, M.). *SLM-Topo – A topology optimization method for additive manufacturing of lightweight design structures using the selective laser melting process*: In: Nafems Nordic Seminar: Exploring the Design Freedom of Additive Manufacturing through Simulation.

[15] Ericson, C. (2008). *Real-Time Collision Detection*. Morgan Kaufmann series in interactive 3D technology: Elsevier Morgan Kaufmann.

[16] Jacobson, A., Kavan, L., and Sorkine-Hornung, O. (2013). *Robust Inside-Outside Segmentation using Generalized Winding Numbers*: In: ACM Trans. Graph. 32, 4. Article 33.

[17] Carneiro, B. P., Silva, C. T., and Kaufman, A. E. (1998). *Tetra-Cubes. An algorithm to generate 3D isosurfaces based upon tetrahedra*.

[18] Spiess, H., Oeckerath, A., and Landvogt, B. (2018). *MapLib Manual. Version 2013.0*.

Acknowledgments

The research documented in this manuscript has been funded by the German Research Foundation (DFG) within the project “SLM-Topo: Development of a process specific topology optimization method for additive manufacturing of lightweight structures exemplified by the SLM process”. The support by the German Research Foundation (DFG) is gratefully acknowledged.